μ-BASED CONTROLLER DESIGN FOR SWITCHING REGULATORS WITH INPUT FILTERS

Michael S. Elmore
E&M Power
6 Emma Street
Binghamton, NY USA
melmore@pronetisp.net

Victor A. Skormin
Electrical and Computer Engineering Department
Binghamton University
Binghamton, NY USA
vskormin@binghamton.edu

Abstract

A switching power supply (SPS) requires an input filter to reduce the high frequency current harmonics generated by switch action that are returned to the source. The interaction between the input filter and control loop of the SPS can adversely affect loop stability, audiosusceptibility and output impedance. To guarantee system stability $Z_s/Z_i + 1$ must satisfy the Nyquist stability criterion, where Z_s is the input filter output impedance and Z_i is the SPS closed-loop input impedance. Parametric uncertainty in the SPS can cause a nominally stable system to become unstable. Component uncertainties **Δ** in the SPS are isolated from the nominal structure **M** and the structured singular value μ is used to analyze robustness of SPS stability with a conventionally designed 2-stage, phase-lead controller with an integrator. It is shown that stability robustness can be improved with a controller designed with a μ-synthesis technique known as D-K iteration. The μ-optimal controller lessens input filter and SPS interactions and improves system stability.

Key Words

Robust Control, Optimal Control, Power Systems, Modeling and Simulation, Stability

1. Introduction

High frequency switching power supply (SPS) input current harmonics are produced by SPS switch action. These current harmonics flow back through the source impedance and create voltage disturbances on the input to the SPS. These voltage disturbances can create problems for the SPS, as well as, other loads on the source bus. High frequency current can find its way to the other loads and cause problems, such as overheating of capacitors and additional input voltage fluctuations. Significant electromagnetic interference problems may arise from high frequency currents traveling through circuit board traces and along cabling.

A filter is usually added to the input of an SPS to reduce the magnitude of the current harmonics injected on the bus. The input filter presents a low impedance to the SPS and keeps current harmonics circulating within the SPS. A well-damped input filter can also benefit the load on the SPS by attenuating high frequency source voltage transients that might otherwise propagate to the output.

However, despite the necessity and benefits of an input filter, an improperly designed input filter can have a detrimental effect on the SPS and destabilize it, especially at lower source voltages and higher loads. The closed-loop, input-to-output transfer characteristic, known as audiosusceptibility and the closed-loop output impedance of the SPS, can also be adversely affected.

1.1 Previous Investigations

Most of the work on the interaction between the input filter and SPS has centered on the proper design of the input filter to meet filtering requirements, while mitigating the adverse effects of the filter on regulator dynamics. The work of Middlebrook [1,2] laid the analytical foundation for understanding the origins of the complex interactions between an input filter and a SPS. This work was founded on the state-space averaging approach of Middlebrook and Ćuk [3] and the canonical circuit models derived from the state-space description of switching power supplies. Middlebrook provided practical, design oriented circuit solutions that were founded on a solid analytical understanding of switching converters. After the unifying work of Middlebrook, researchers started taking a more detailed look at optimization of input filters [4,5]. Development of practical design guidelines for input filters that did not result in adverse interactions with the SPS was a goal.

There has also been research on the proper design of the SPS to reduce interactions with the input filter. Middlebrook has discussed the use of lossless damping to reduce the peaking of the SPS output filter [6]. While Middlebrook's approach introduces additional, low-loss power train components to dampen the peaking, others have pursued small-signal approaches. Current programmed SPS and their interactions with input filters

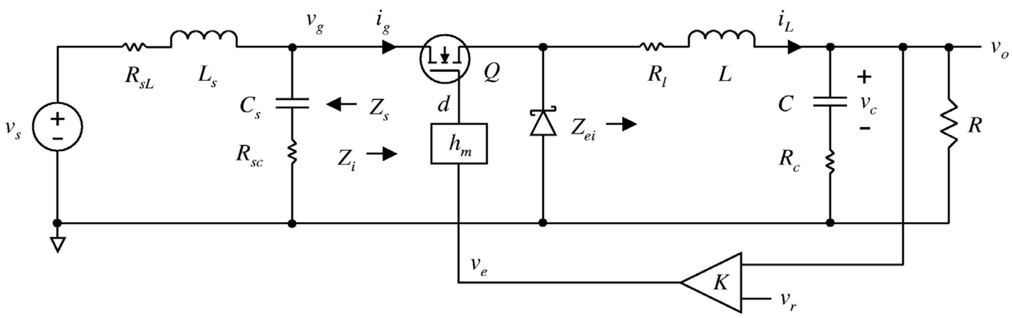

Fig. 1 – Buck Converter with Input Filter and Controller

have been investigated extensively [7, 8, 9]. A common point made throughout these studies is the effectiveness of current mode control to dampen the peaking of the SPS output filter. The reduced peaking lowers the input admittance of the SPS and leads to less interaction between the SPS and input filter. Novel adaptive control methods have also been utilized to reduce input filter and SPS interactions [10, 11, 12], although these control methods tend to be complex and do more than just lessen interactions between the input filter and SPS.

1.2 Scope of the Current Work

The current work presents a μ-synthesis design approach to reduce the closed-loop input admittance of a SPS in its mid-frequency range and mitigate input filter interactions. The uncertainty $\boldsymbol{\Delta}$ in individual power train components is separated from the nominal structure **M** of a SPS and a linear fractional representation of the system is constructed. The component uncertainty block $\boldsymbol{\Delta}$ is augmented with a performance uncertainty block $\boldsymbol{\Delta}_p$ that represents exogenous disturbances to the system. With the augmented uncertainty structure, perturbations to the SPS components, input voltage, and regulation reference voltage can be used to design a robust controller, which minimizes closed-loop input admittance and maintains acceptable gain and phase margins for stability.

A robust, optimal controller for a buck converter with an input filter is designed with the Matlab μ-Analysis and Synthesis [13], LMI Control [14], and Linear Fractional Representation [15] toolboxes. Simulation results are given for robust stability and performance μ, closed-loop input impedance, and open-loop gain. A Nyquist stability analysis is done to evaluate the input filter and buck interactions. All simulation results with the robust, optimal controller are compared to results with a conventionally designed 2-stage, phase-lead controller with an integrator.

2. Theoretical Background

In the following discussion signals are represented in their steady-state X, small signal $\hat{x}$, or total $x = X + \hat{x}$ forms, as appropriate. Transfer functions are represented with italicized capital letters. Vector and matrix quantities are represented with bold capital letters. All converter performance characteristics are closed-loop, unless otherwise stated.

2.1 Converter Small Signal Modeling

Middlebrook and Ćuk [3] have developed small-signal, low frequency models of standard switching converter topologies: 1) buck, 2) boost, and 3) buck-boost. The models represent an average over one switch cycle of the on and off states of converters operating in the continuous mode. Such a model can be used to investigate the effects of parameter variation on converter performance characteristics, such as stability, audiosusceptibility, and input and output impedances. Small signal descriptor state (1) and output (2) equations below represent the buck converter in Fig. 1. The state variable $\hat{\mathbf{x}} = \begin{bmatrix} \hat{i}_L & \hat{v}_c \end{bmatrix}^{\mathrm{T}}$ consists of the inductor current $\hat{i}_L$ and capacitor voltage $\hat{v}_c$. The input $\hat{\mathbf{u}} = \begin{bmatrix} \hat{v}_g & \hat{v}_e \end{bmatrix}^{\mathrm{T}}$ consists of the input $\hat{v}_g$ and control $\hat{v}_e$ voltages, where $\hat{d} = h_m \cdot \hat{v}_e$. $\hat{d}$ is the converter duty cycle and h_m is the modulator gain. The modulator converts the analog signal $\hat{v}_e$ to a pulsed voltage to switch Q between the on and off states. The output is $\hat{\mathbf{y}} = \begin{bmatrix} \hat{i}_g & \hat{v}_o \end{bmatrix}^{\mathrm{T}}$, where $\hat{i}_g$ is the buck input current and $\hat{v}_o$ is the output voltage. The small signal descriptor state space (DSS) equation is

$$\mathbf{E} \cdot \dot{\hat{\mathbf{x}}} = \mathbf{A} \cdot \hat{\mathbf{x}} + \mathbf{B} \cdot \hat{\mathbf{u}}\,, \tag{1}$$

where $\mathbf{A} = \begin{bmatrix} -R_l - R \| R_c & -\dfrac{R}{R+R_c} \\ \dfrac{R}{R+R_c} & -\dfrac{1}{R+R_c} \end{bmatrix}$, $\mathbf{B} = \begin{bmatrix} D & V_g \cdot h_m \\ 0 & 0 \end{bmatrix}$,

and $\mathbf{E} = \begin{bmatrix} L & 0 \\ 0 & C \end{bmatrix}$. The output equation is

$$\hat{\mathbf{y}} = \mathbf{C} \cdot \hat{\mathbf{x}} + \mathbf{D} \cdot \hat{\mathbf{u}}\,, \tag{2}$$

where $\mathbf{C} = \begin{bmatrix} D & 0 \\ R \| R_c & \dfrac{R}{R+R_c} \end{bmatrix}$ and $\mathbf{D} = \begin{bmatrix} 0 & \dfrac{D \cdot V_g \cdot h_m}{R} \\ 0 & 0 \end{bmatrix}$.

2.2 Input Filter Interactions

A requirement for system stability of the buck converter and filter in Fig. 1 is that $T_1 + 1$, where $T_1 = Z_s / Z_i$ is a minor loop gain, does not have any roots in the right half plane (RHP). In other words $T_1 + 1$ must satisfy the Nyquist stability criterion. The SPS input impedance Z_i is best described with the input admittance Y_i, which is

$$Y_i = \frac{1}{Z_i} = -\frac{T}{1+T} \cdot \frac{D^2}{R} + \frac{1}{1+T} \cdot \frac{D^2}{Z_{ei}}, \tag{3}$$

where T is the buck and controller loop gain and Z_{ei} is the input impedance of the buck output filter. (3) is derived from the *canonical circuit model* [3], which is a circuit realization of the state space model in (1) and (2). Z_{ei} may possess significant peaking in its mid-frequency range and result in low phase or gain stability margins or even instability in either T_1 or the major loop T. Uncertainty in converter components results in a widely varying Z_{ei} and makes it difficult to meet performance objectives and maintain stability. However, optimum design of the controller K can reduce the peaking, improve stability margins, or even turn an unstable system into a stable one.

2.3 Linear Fractional Representation

A matrix **M**, relating input $\mathbf{u} = [\mathbf{u}_1; \mathbf{u}_2]$ and output $\mathbf{p} = [\mathbf{p}_1; \mathbf{p}_2]$, can be partitioned into top and bottom parts, so that $\mathbf{p}_1 = \mathbf{M}_{11} \cdot \mathbf{u}_1 + \mathbf{M}_{12} \cdot \mathbf{u}_2$ and $\mathbf{p}_2 = \mathbf{M}_{21} \cdot \mathbf{u}_1 + \mathbf{M}_{22} \cdot \mathbf{u}_2$. If a second matrix $\mathbf{\Delta}$ is introduced, so that $\mathbf{u}_1 = \mathbf{\Delta} \cdot \mathbf{p}_1$, then the relationship between $\mathbf{u}_2$ and $\mathbf{p}_2$ can be solved to give

$$\mathbf{p}_2 = \left[\mathbf{M}_{22} + \mathbf{M}_{21} \cdot \mathbf{\Delta} \cdot (\mathbf{I} - \mathbf{M}_{11} \cdot \mathbf{\Delta})^{-1} \cdot \mathbf{M}_{12}\right] \cdot \mathbf{u}_2$$

or

$$\mathbf{p}_2 = F_U(\mathbf{M} \cdot \mathbf{\Delta}) \cdot \mathbf{u}_2 . \tag{4}$$

$F_U(\mathbf{M} \cdot \mathbf{\Delta})$ is an *upper* linear fractional representation (LFR) or transformation. If $\mathbf{\Delta}$ is introduced, so that $\mathbf{u}_2 = \mathbf{\Delta} \cdot \mathbf{p}_2$, then the relationship between $\mathbf{u}_1$ and $\mathbf{p}_1$ can be solved for a *lower* LFR $F_L(\mathbf{M} \cdot \mathbf{\Delta})$. Uncertain systems can be structured as a LFR, in which **M** represents the nominal system and $\mathbf{\Delta}$ the system uncertainty.

Each of the five components L, C, R, R_l, and R_c in (1) and (2) have some uncertainty. The uncertainty can be represented as an *additive* perturbation $p = p_n \pm \Delta p$, where p_n is the nominal component value and Δp is the perturbation from p_n. The parametric uncertainty must be separated from the nominal system to perform μ-analysis and synthesis. This is a difficult task for some systems. Buso [16] modeled the parametric uncertainty in a buck-boost converter as two lumped, complex *multiplicative* perturbations, which are easily structured as a linear fractional representation (LFR). This approach does not allow the uncertainty in individual components to be investigated. Tymerski [17] created a LFR which used both additive and multiplicative perturbations to model individual component uncertainties. However, the conversion from the state space representation to the LFR is difficult and requires some intuition on the part of the designer.

More recently Gahinet [14] has provided a systematic approach to separating parametric uncertainty from an uncertain system in descriptor state space (DSS) form. The technique requires that the uncertain DSS form be transformed to an intermediate affine parameter dependent system, which can then easily be converted to a LFR.

Uncertain linear systems with affine parameter dependence can be expressed in descriptor state space (DSS) form as

$$\begin{bmatrix} \mathbf{E}_n & \mathbf{0} \\ \mathbf{0} & \mathbf{I} \end{bmatrix} \cdot \begin{bmatrix} \dot{\mathbf{x}} \\ \mathbf{y} \end{bmatrix} = \begin{bmatrix} \mathbf{A}_n & \mathbf{B}_n \\ \mathbf{C}_n & \mathbf{D}_n \end{bmatrix} \cdot \begin{bmatrix} \mathbf{x} \\ \mathbf{u} \end{bmatrix} + \sum_{i=1}^{m} \boldsymbol{\delta}_i \cdot \mathbf{P}_i \cdot \begin{bmatrix} \dot{\mathbf{x}} \\ \mathbf{x} \\ \mathbf{u} \end{bmatrix}, \tag{5}$$

where $\mathbf{P}_i = \begin{bmatrix} -\mathbf{E}_i & \mathbf{A}_i & \mathbf{B}_i \\ \mathbf{0} & \mathbf{C}_i & \mathbf{D}_i \end{bmatrix}$ and m is the number of uncertain parameters. Each $\boldsymbol{\delta}_i = \delta_i \cdot \mathbf{I}_{ri}$ represents a system component and each element of $\mathbf{P}_i$ is a constant matrix. $\mathbf{I}_{ri}$ is an identity matrix of dimension $r_i \times r_i$. The subscript n signifies a matrix with nominal component values. Singular value decomposition is used to factor each $\mathbf{P}_i$ to give

$$\begin{bmatrix} -\mathbf{E}_i & \mathbf{A}_i & \mathbf{B}_i \\ \mathbf{0} & \mathbf{C}_i & \mathbf{D}_i \end{bmatrix} = \begin{bmatrix} \mathbf{L}_i \\ \mathbf{M}_i \end{bmatrix} \cdot [\mathbf{T}_i \quad \mathbf{R}_i \quad \mathbf{S}_i] . \tag{6}$$

The factors are accumulated in matrices **L**, **M**, **T**, **R**, and **S**.

The goal of the intermediate transformation in (6) is to create a LFR such that

$$\mathbf{E}_n \cdot \dot{\mathbf{x}} = \mathbf{A}_n \cdot \mathbf{x} + \mathbf{B}_{zx} \cdot \mathbf{w} + \mathbf{B}_n \cdot \mathbf{u} ,$$
$$\mathbf{z} = \mathbf{C}_{xw} \cdot \mathbf{x} + \mathbf{D}_{zw} \cdot \mathbf{w} + \mathbf{D}_{uw} \cdot \mathbf{u} ,$$

and

$$\mathbf{y} = \mathbf{C}_n \cdot \mathbf{x} + \mathbf{D}_{zy} \cdot \mathbf{w} + \mathbf{D}_n \cdot \mathbf{u}, \tag{7}$$

where $\mathbf{w} = \mathbf{\Delta} \cdot \mathbf{z}$. (7) is illustrated in Fig. 2. The system matrix **M** and uncertainty matrix $\mathbf{\Delta}$ are shown. After some algebra, it can be shown [18] that $\mathbf{B}_{zx} = \mathbf{L}$, $\mathbf{C}_{xw} = \mathbf{R} - \mathbf{T} \cdot \mathbf{E}_n^{-1} \cdot \mathbf{A}_n$, $\mathbf{D}_{zw} = -\mathbf{T} \cdot \mathbf{E}_n^{-1} \cdot \mathbf{L}$, $\mathbf{D}_{zy} = \mathbf{M}$,

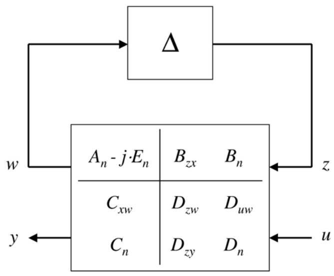

Fig. 2 – LFR for Descriptor State Space System

and $\mathbf{D}_{uw} = \mathbf{S} - \mathbf{T} \cdot \mathbf{E}_n^{-1} \cdot \mathbf{B}_n$.

For μ-analysis and synthesis the parameter variations δ should be normalized to δ′ so that δ′∈[-1 1]. This can be accomplished with a transformation

$$\mathbf{\Delta} = \mathbf{R} + \mathbf{P} \cdot \mathbf{\Delta}' \cdot \mathbf{Q}\,, \tag{8}$$

where $\mathbf{P} = diag\left(\mathbf{I}_{r_1}, \ldots, \mathbf{I}_{r_m}\right)$,

$$\mathbf{R} = diag\left(\mathbf{I}_{r_1} \cdot \frac{\delta_1^+ + \delta_1^-}{2}, \ldots, \mathbf{I}_{r_m} \cdot \frac{\delta_m^+ + \delta_m^-}{2}\right),$$

and $$\mathbf{Q} = diag\left(\mathbf{I}_{r_1} \cdot \frac{\delta_1^+ - \delta_1^-}{2}, \ldots, \mathbf{I}_{r_m} \cdot \frac{\delta_m^+ - \delta_m^-}{2}\right).$$

It can be shown [15] that $F_u(\mathbf{M}, \mathbf{\Delta}) = F_u(\mathbf{M}', \mathbf{\Delta}')$, where

$$\mathbf{M}'_{11} = \mathbf{Q} \cdot (\mathbf{I} - \mathbf{M}_{11} \cdot \mathbf{R})^{-1} \cdot \mathbf{M}_{11} \cdot \mathbf{P}\,,$$

$$\mathbf{M}'_{12} = \mathbf{Q} \cdot (\mathbf{I} - \mathbf{M}_{11} \cdot \mathbf{R})^{-1} \cdot \mathbf{M}_{12}\,,$$

$$\mathbf{M}'_{21} = \mathbf{M}_{21} \cdot \mathbf{P} + \mathbf{M}_{21} \cdot \mathbf{R} \cdot (\mathbf{I} - \mathbf{M}_{11} \cdot \mathbf{R})^{-1} \cdot \mathbf{M}_{11} \cdot \mathbf{P}\,,$$

and $$\mathbf{M}'_{22} = \mathbf{M}_{22} + \mathbf{M}_{21} \cdot \mathbf{R} \cdot (\mathbf{I} - \mathbf{M}_{11} \cdot \mathbf{R})^{-1} \cdot \mathbf{M}_{12}\,. \tag{9}$$

2.4 μ -Analysis and Synthesis

The structured singular value is defined as

$$\mu_{\mathbf{\Delta}}(\mathbf{M}) = \frac{1}{\min\left\{\bar{\sigma}(\Delta) : \Delta \in \mathbf{\Delta}, \det(\mathrm{I} - \Delta \cdot \mathbf{M}) = 0\right\}}\,, \tag{10}$$

unless no $\Delta \in \mathbf{\Delta}$ makes **I** - **M**·**Δ** singular, in which case $\mu_\Delta(\mathbf{M}) := 0$. $\bar{\sigma}(\mathbf{\Delta})$ is the maximum singular value of the uncertainty block and $\mathbf{\Delta} = \{diag\left(\delta_1^r \cdot \mathbf{I}_{r_1}, \ldots, \delta_{m_r}^r \cdot \mathbf{I}_{r_{m_r}}, \delta_1^c \cdot \mathbf{I}_{r_{m_r+1}}, \ldots, \delta_{m_c}^c \cdot \mathbf{I}_{r_{m_r+m_c}}, \Delta_1, \ldots, \Delta_{m_C}\right) : \delta_i^r \in \mathrm{R}, \delta_i^c \in \mathrm{C}, \Delta_i \in \mathrm{C}^{r_{m_r+m_c+i} r_{m_r+m_c+i}}\}$. The structured singular value $\mu_\Delta(\mathbf{M})$ is used to analyze the robustness of systems. Calculation of $\mu_\Delta(\mathbf{M})$ is an NP hard problem, however, algorithms have been created to find upper β_u and lower β_ℓ bounds of $\mu_\Delta(\mathbf{M})$ across a frequency range of interest. β_u separates the results into regions that are guaranteed robustly stable and not robustly stable. β_ℓ provides a measure of the possible conservativeness of the results.

Performance criteria, such as input impedance and tracking error, can be evaluated by incorporating exogenous signals into the system. In the case of input impedance Z_i the signals have already been included in (1) and (2). The small signal input impedance can also be defined as

$$Z_i = \frac{\hat{v}_g}{\hat{i}_g}\,, \tag{11}$$

where $\hat{v}_g$ is the buck input voltage and $\hat{i}_g$ is the buck input current. The small signal tracking error is defined as

$$\hat{e} = \hat{v}_r - \hat{v}_o\,, \tag{12}$$

where $\hat{v}_o$ is the buck output voltage. $\hat{v}_r$ is the regulation reference voltage. These criteria can be evaluated by introducing a disturbance on one signal and measuring its effect on the other. For example, if a disturbance is introduced on the input voltage $\hat{v}_g$, the effect on the input current $\hat{i}_g$ can be measured and their ratio taken to determine the input impedance Z_i. Furthermore, if the input current is weighted with the expected or desired input impedance, then the input impedance is essentially normalized. The parametric uncertainty block **Δ** can be augmented with a performance uncertainty block $\mathbf{\Delta}_p$ that represents these performance or exogenous disturbances. $\mu_\Delta(\mathbf{M})$ can then be used to evaluate the effect of the augmented uncertainty block *diag* ($\mathbf{\Delta}$, $\mathbf{\Delta}_p$) on the system **M**. In this manner the performance criteria are evaluated in the context of their effect on system "stability".

μ-synthesis consists of finding a controller that minimizes $\mu_\Delta(\mathbf{M})$ across a range of frequencies. Minimization of $\mu_\Delta(\mathbf{M})$ implies that a larger set of perturbations in *diag* ($\mathbf{\Delta}$, $\mathbf{\Delta}_p$) is necessary to drive the system into instability. In this sense the controller is "optimum". An algorithm known as D-K iteration is used to find the optimum controller. D refers to scaling matrices that are used in μ-analysis and synthesis to calculate the upper bound β_u on $\mu_\Delta(\mathbf{M})$. K refers to the controller. For a fixed **D** finding the *K* that minimizes $\mu_\Delta(\mathbf{M})$ is a standard H_∞ control problem. For a given stabilizing *K* finding a new **D** that minimizes $\mu_\Delta(\mathbf{M})$ is a standard convex optimization problem. The D-K iteration proceeds back and forth between these two parameter minimizations, until an acceptable error between iterations is reached. With arguments based on the *small gain theorem* it can be shown that the condition for robust stability is $\mu_\Delta(\mathbf{M}_{11}(j \cdot \omega)) < 1 \ \forall\ \omega$. Robust performance is achieved, if $\mu_\Delta(\mathbf{M}(j \cdot \omega)) < 1 \ \forall\ \omega$.

3. Results For Buck Converter

The buck topology in Fig. 1 is selected to investigate converter interactions with a single stage input filter. The nominal component values of the buck are L = 1.80μH, C = 1750μF, R = 1Ω, R_l = 30mΩ, and R_c = 9mΩ. The uncertainty in each component is ±50%. The input voltage to the buck is V_g = 12V and the output voltage V_o = 5V. This results in a static duty cycle $D \approx 0.417$. The modulator gain is h_m = 0.511. The modulator gain is dependent on the particular circuit implementation that is chosen. The input filter component values are L_s = 3.20μH, C_s = 48μH, R_{sL} = 30mΩ, and R_{cs} = 0.3mΩ.

3.1 Converter Representation

The parametric uncertainty in the buck converter in (1) and (2) is represented as an affine parameter dependent system. It is assumed that $R_c << R$. This does not result in any significant effect on the system and is true for most buck converter designs. The **A**, **C**, **D**, and **E** system matrices become

$$\mathbf{A}_d = \begin{bmatrix} 0 & -1 \\ 1 & 0 \end{bmatrix} + \begin{bmatrix} -1 & 0 \\ 0 & 0 \end{bmatrix} \cdot R_l + \begin{bmatrix} -1 & 0 \\ 0 & 0 \end{bmatrix} \cdot R_c + \begin{bmatrix} 0 & 0 \\ 0 & -1 \end{bmatrix} \cdot G,$$

$$\mathbf{C}_d = \begin{bmatrix} D & 0 \\ 0 & 1 \end{bmatrix} + \begin{bmatrix} 0 & 0 \\ 1 & 0 \end{bmatrix} \cdot R_c,$$

$$\mathbf{D}_d = \begin{bmatrix} 0 & D \cdot V_g \cdot h_m \\ 0 & 0 \end{bmatrix} \cdot G,$$

and

$$\mathbf{E}_d = \begin{bmatrix} 1 & 0 \\ 0 & 0 \end{bmatrix} \cdot L + \begin{bmatrix} 0 & 0 \\ 0 & 1 \end{bmatrix} \cdot C, \tag{13}$$

where $G = 1/R$. Each constant matrix is an element of $\mathbf{P}_i$ in (6). The $\mathbf{B}_d = \mathbf{B}$ matrix is unchanged, because it does not depend on any component parameter. The subscript d is a reminder that $R_c << R$.

The weighting function for the input current is

$$W_{z_i} = 0.1688 \cdot \frac{\frac{s}{2000} + 1}{\left[\frac{s}{20000} + 1\right]^2}. \tag{14}$$

W_{z_i} represents the desired input impedance Z_i and shapes the small signal closed-loop input current $\hat{i}_g$, so that $\left\| W_{z_i} \cdot \hat{i}_g \right\| < 1$, as in any standard H_∞ control problem. Complex perturbations from the uncertainty block **Δ** are injected on the buck input voltage to produce $\hat{i}_g$. At low frequency W_{z_i} is equivalent to the buck converter input impedance with nominal component values. In the mid-frequency range, where the controller is able to modify Z_i, W_{z_i} has been selected to raise the buck input impedance. Stability gain and phase margins cannot be controlled with only W_{z_i}, so a second weighting function W_e for the tracking error is defined. It is

$$W_e = 50000 \cdot \frac{\frac{s}{20000} + 1}{\left[\frac{s}{0.5} + 1\right] \cdot \left[\frac{s}{10000} + 1\right]}. \tag{15}$$

The descriptor state space model in (1) and (2), the ±50% parametric uncertainty, and the weighting functions in (14) and (15) are implemented in Matlab. Functions in the LMI Control [14] and Linear Fractional Representation [15] toolboxes are used to create the affine model, convert it to a LFR, and normalize the parametric uncertainty. The performance objectives for input impedance and stability phase and gain margins are implemented as exogenous disturbances in $\mathbf{\Delta}_p$ and added to the normalized parametric uncertainty block **Δ**, resulting in $diag(\mathbf{\Delta}, \mathbf{\Delta}_p)$.

The μ-Analysis and Synthesis [13] toolbox is used to perform D-K iteration and create an optimum controller K_{OPT}. The optimum controller has order 18. It is reduced to order 3 with a truncated balanced realization. The transfer function of the reduced order controller is

$$K_{OPT} = -\frac{4697 \cdot \left[\frac{s}{2.12 \cdot 10^7} - 1\right] \cdot \left[\frac{s}{5610} + 1\right]^2}{\left[\frac{s}{.5} + 1\right] \cdot \left[\frac{s}{5.16 \cdot 10^4} + 1\right] \cdot \left[\frac{s}{5.86 \cdot 10^5} + 1\right]}. \tag{16}$$

K_{OPT} is plotted in Fig. 3, along with the non-reduced controller, and a non-optimum, 2-stage, phase-lead controller K with an integrator, designed mostly by trial and error with frequency domain analysis. It can be seen that the reduced order, optimum controller follows the non-reduced, optimum controller closely. The obvious benefit from the optimum controller is improved gain and phase in the middle to high frequency range.

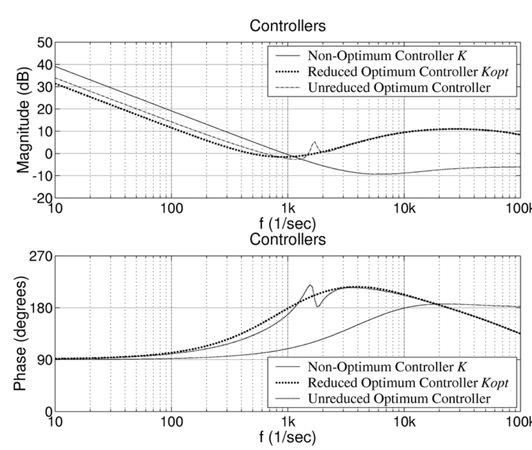

Fig. 3 – Controller Comparison

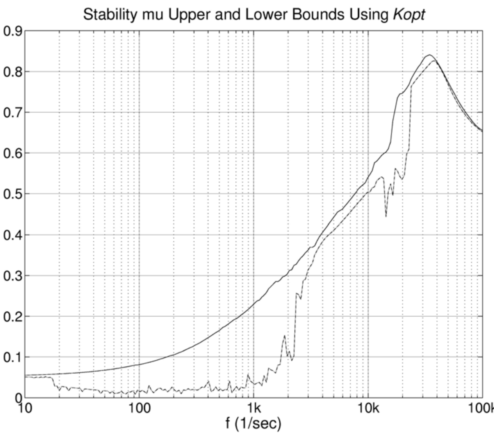

Fig. 4 – μ for Stability

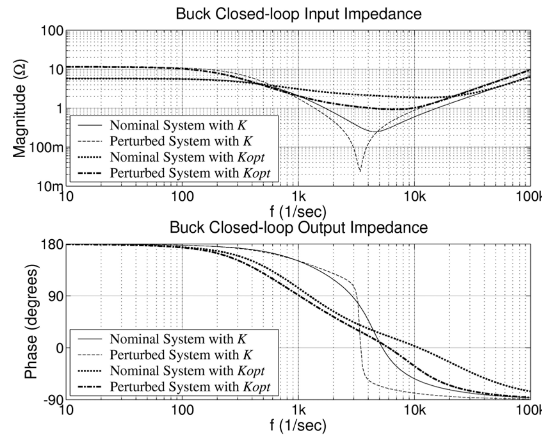

Fig. 6 – Closed-Loop Input Impedance

μ-analysis for stability is shown in Fig. 4. This analysis shows that the buck is stable for component variations of ±50%, since $\mu_\Delta(\mathbf{M}_{11}) < 1 \ \forall f$. The real valued parametric uncertainty block $\mathbf{\Delta}$ is weighted with a small percentage (10%) of complex valued uncertainty to give a lower bound β_ℓ that converges reasonably well. This weighting makes the bounds somewhat more conservative, although stability is still achieved for the entire range of uncertainty.

μ-analysis for performance is shown in Fig. 5. This analysis shows that the buck does not achieve robust performance, since $\mu_\Delta(\mathbf{M}) > 1$ at middle to lower frequencies. This is because the weighting function W_{z_i} in (14) is not entirely met. To emphasize its role in shaping input impedance W_{z_i} is chosen to have the shape of the desired nominal, damped input impedance. Since the controller has no effect on low frequency input impedance, parametric perturbations mean $\left\| W_{z_i} \cdot \hat{i}_g \right\| < 1$ cannot be guaranteed. Nevertheless, the mid-frequency peaking in the input impedance has been significantly decreased with the reduced, optimum controller, as can be seen in Fig. 6. Nominal and perturbed buck converter input impedance with both the non-optimum and reduced, optimum controllers are shown. The component perturbations consist of a 50% increase in L and C and a 50% reduction in R_l and R_c from the nominal values. Other combinations of component variations within the specified ±50% show similar reductions in peaking.

Fig. 7 shows the nominal and perturbed buck open-loop gain with the same component variations. It can be seen that the bandwidth has increased with the reduced, optimum controller and the phase margin has been improved, especially for the perturbed system. The increased bandwidth is not a problem, provided the converter switch frequency is not too low. 200 – 300kHz is acceptable. Fig. 8 shows the Nyquist stability analysis of the combined input filter and buck converter with both the non-optimum and the reduced, optimum controller. The component variations are the same, as before. The ratio of the output impedance of the input filter to the input impedance of the buck with the non-optimum controller Z_S / Z_{Ci} encircles (-1, j0), indicating that the system is unstable. However, the ratio of the output impedance of the input filter to the input impedance of the buck with the reduced, optimum controller Z_S / Z_{r_i} does not encircle (-1, j0), indicating that the system is stable with good phase margin.

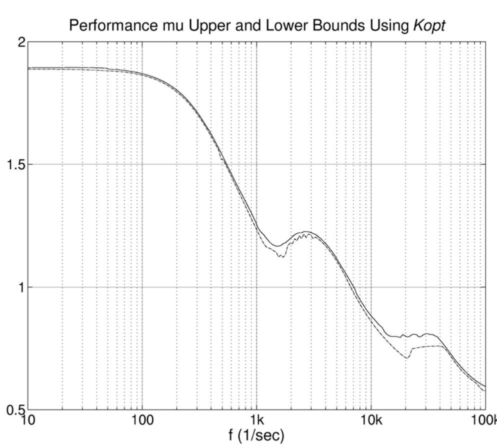

Fig. 5 – μ for Performance

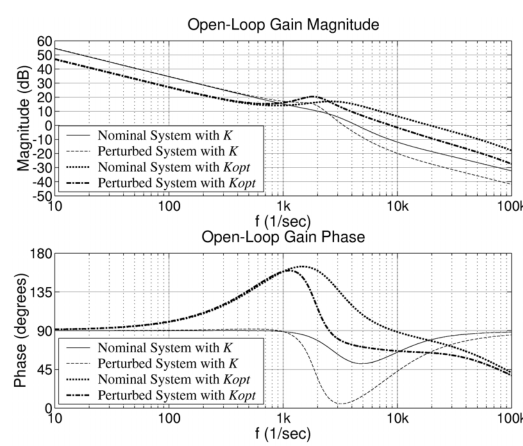

Fig. 7 – Open-Loop Gain

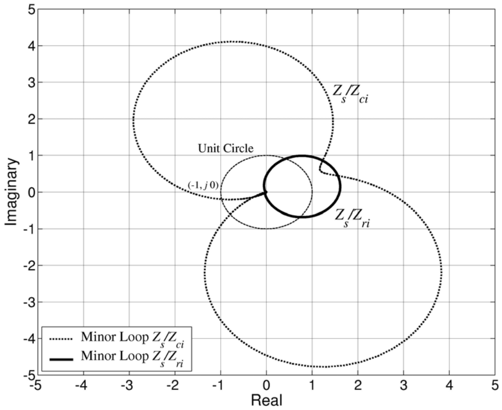

Fig. 8 – Nyquist Stability for Minor Loop Gain T_1

4. Conclusions

Parametric uncertainty in a buck converter is modeled in a linear fractional representation (LFR). The construction of the LFR from the descriptor state space (DSS) form is facilitated with an intermediate affine parameter dependent representation. Converter input impedance and stability margins are specified in weighting functions and included with parametric perturbations in an augmented uncertainty block.

A μ-optimum controller is designed with D-K iteration and shown to increase the input impedance of a buck converter by reducing the peaking effects of the output filter. This eliminates an instability in the minor loop gain $T_1 = Z_s / Z_i$ between the converter input filter and the converter with ±50% variation in converter power train component values.

References

[1] R. Middlebrook, Input filter considerations in design and application of switching regulators, *Proc. IEEE Industry Applicat. Soc. Annual Meeting*, Chicago, IL, 1976, 366 – 382.

[2] R. Middlebrook, Design techniques for preventing input-filter oscillations in switched-mode regulators, *Proc. 5th Int. Solid State Power Conversion Conf.*, San Francisco, CA, 1978, A3-1 – A3-16.

[3] R. Middlebrook and S. Ćuk, General unified approach to modelling switching-converter power stages, *International Journal of Electronics*, *42*(6), 1977, 521 – 550.

[4] T. Phelps and W. Tate, Optimizing Passive Input Filter Design, *Proc. of the 6th National Solid-State Power Conversion Conf.*, Miami Beach, FL, 1979, G1-1 – G1-10.

[5] F. Lee and Y. Yu, Input-filter design for switching regulators, *IEEE Trans. on Aerospace and Electron. Systems*, *AES-15*(5), 1979, 627 – 634.

[6] R. Middlebrook, Power filter damping, *Proc. IEEE Power Electron. Specialist Conf.*, Anaheim, CA, 1985, 96 – 105.

[7] S. Erich and W. Polivka, Input filter design criteria for current-programmed converters, *IEEE Trans. on Power Electron.*, *7*(1), 1992, 143 – 151.

[8] Y. Jang and R. Erickson, Physical origins of input filter oscillations in current programmed converters, *IEEE Trans. on Power Electron.*, *7*(4), 1992, 725 – 733.

[9] T. Suntio, I. Gaoura, and K. Zenger, Input filter interactions in peak-current-mode-controlled buck converter operating in CICM, *IEEE Trans. on Power Electron.*, *49*(1), 2002, 76 – 86.

[10] S. Kelkar and F. Lee, Adaptive input filter compensation for switching regulators, *IEEE Trans. on Aerospace and Electron. Systems*, *AES-20*(1), 1984, 57 – 66.

[11] S. Kelkar and F. Lee, A novel input filter compensation scheme for switching regulators, *Proc. of the IEEE Power Electron. Specialists Conf.*, Cambridge, MA, 1982, 260 – 271.

[12] M. Elmore, C. Ellison, and V. Skormin, Adaptive model following control for switching regulators with input filters, *Proc. 29th Annual Conf. of the IEEE Industrial Electron. Soc.*, Roanoke, VA, 2003, 562 – 567.

[13] G. Balas, J. Doyle, et al, *μ analysis and synthesis toolbox user's guide, ver. 3*, (Natick, MA, The Math Works, Inc., 1998).

[14] P. Gahinet, A. Nemirovski, et al, *LMI control toolbox user's guide* (Natick, MA, The Math Works, Inc., 1995).

[15] J. –F. Magni, *Linear fractional representation toolbox: modelling, order reduction, gain scheduling* (http://www.cert.fr/dcsd/idco/perso/Magni/booksandtb.html#LFRT, 2004).

[16] S. Buso, Design of a robust voltage controller for a buck-boost converter using μ-synthesis, *IEEE Trans. on Control Systems Technology*, *7*(2), 1999, 222 – 229.

[17] R. Tymerski, Worst-case stability analysis of switching regulators using the structured singular value, *IEEE Trans. on Power Electron.*, *11*(5), 1996, 723 – 730.

[18] P. Gahinet, personal correspondence, Mar. 2004.